BIOCHEMISTRY
including biophysical chemistry & molecular biology

Article

pubs.acs.org/biochemistry

Detergent-Type Membrane Fragmentation by MSI-78, MSI-367, MSI-594, and MSI-843 Antimicrobial Peptides and Inhibition by Cholesterol: A Solid-State Nuclear Magnetic Resonance Study

Dong-Kuk Lee,[†,‡] Anirban Bhunia,[†,§] Samuel A. Kotler,[†] and Ayyalusamy Ramamoorthy*[,†]

[†]Biophysics and Department of Chemistry, University of Michigan, Ann Arbor, Michigan 48109-1055, United States

[‡]Department of Fine Chemistry & Convergence Institute of Biomedical and Biomaterials, Seoul National University of Technology, Seoul 139-743, Korea

[§]Department of Biophysics, Bose Institute, P-1/12 CIT Scheme VII(M), Kolkata 700054, India

Supporting Information

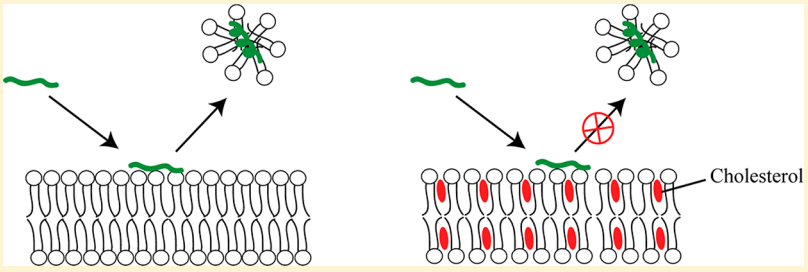

ABSTRACT: Multidrug resistance against the existing antibiotics is becoming a global threat, and any potential drug that can be designed using cationic antimicrobial peptides (AMP) could be an alternate solution to alleviate this existing problem. The mechanism of action of killing bacteria by an AMP differs drastically in comparison to that of small molecule antibiotics. The main target of AMPs is to interact with the lipid bilayer of the cell membrane and disrupt it to kill bacteria. Consequently, the modes of membrane interaction that lead to the selectivity of an AMP are very important to understand. Here, we have used different membrane compositions, such as negatively charged, zwitterionic, or mixed large unilamellar vesicles (LUVs), to study the interaction of four different synthetically designed cationic, linear antimicrobial peptides: MSI-78 (commercially known as pexiganan), MSI-367, MSI-594, and MSI-843. Our solid-state nuclear magnetic resonance (NMR) experiments confirmed that the MSI peptides fragmented LUVs through a detergent-like carpet mechanism depending on the amino acid sequence of the MSI peptide and/or the membrane composition of LUVs. Interestingly, the fragmented lipid aggregates such as SUVs or micelles are sufficiently small to produce an isotropic peak in the ^{31}P NMR spectrum. These fragmented lipid aggregates contain only MSI peptides bestowed with lipid molecules as confirmed by NMR in conjunction with circular dichroism spectroscopy. Our results also demonstrate that cholesterol, which is present only in the eukaryotic cell membrane, inhibits the MSI-induced fragmentation of LUVs, suggesting that the MSI peptides can discriminate the bacteria and the eukaryotic cell membranes, and this selectivity could be used for further development of novel antibiotics.

The classical antibiotic era against life-threatening diseases may be coming to an end because of multidrug resistance (MDR), and this fact is quickly becoming a burning problem in medical sciences. Therefore, there is an urgent need for new types of pharmaceutical compounds for treating bacterial infections. In this regard, antimicrobial peptides (AMPs) offer the prospect of becoming the next generation of antibiotic compounds. AMPs are the key components of innate immunity, present in all forms of life, and are bestowed with a broad spectrum of antimicrobial activities. The amino acid composition of AMPs consists of both hydrophobic and cationic residues.[1,2] Because of unique amino acid sequences, most AMPs kill bacteria by directly interacting with the anionic lipid bilayer of a bacterial cell membrane and subsequently inserting into its hydrophobic core leading to disruption of the lipid bilayer structure.[3−7] There is significant fundamental interest in understanding the mechanism of AMP-induced cell death due to the ability of AMPs to selectively[8] and directly interact with the lipid components of a bacterial cell membrane.[9−13] Such information would aid in the design of efficient AMPs and is considered to be a key element in avoiding bacterial resistance.

The selectivity of an AMP for a prokaryotic cell membrane (as opposed to a eukaryotic cell membrane) is an important aspect of AMP activity that can be utilized in the design of potent AMPs.[14−16] Interestingly, a bacterial cell membrane consists of negatively charged lipids, whereas a eukaryotic cell membrane is comprised of a variety of lipids, including, but not

Received: November 14, 2014
Revised: February 10, 2015
Published: February 25, 2015

DOI: 10.1021/bi501418m
Biochemistry 2015, 54, 1897−1907

limited to, zwitterionic lipids, acidic lipids, glycolipids, and cholesterol.[17] Furthermore, the distribution of acidic lipids in a eukaryotic membrane is highly disordered and very complex in nature. Conversely, a number of studies using various biochemical approaches and biophysical techniques, including sophisticated solid-state NMR techniques,[18] showed that cholesterol increases the level of membrane order and suppresses the membrane disrupting action of an AMP.[19,20] Extensive studies have also been reported for the complex, heterogeneous lipid vesicles containing cholesterol and its effect on the function of AMPs.[21] In a recent study, it was found that cholesterol alters membrane disruption by AMPs,[22,23] whereas another study has shown that cholesterol present in raft-containing membranes does not play a significant role in determining the selectivity of AMPs.[8,19,21] However, a systematic investigation of the role of cholesterol, membrane composition, and amino acid sequence of AMPs would be useful for understanding the different types of mechanisms of action of AMPs.

Genaera Corp. initially designed a series of AMPs, called MSI peptides, in which the design principle utilized the amino acid sequences of magainin and melittin and also used non-natural amino acids like ornithine. Some of these MSI peptides are used in this study (Table 1). One of the MSI peptides, MSI-78 (or commercially known as pexiganan), reached phase II clinical trials to treat infection of diabetic foot ulcers.[24,25] Though the net charge of these MSI peptides is not the same, they exhibit a broad range of antimicrobial activities against Gram-positive as well as Gram-negative bacteria.[26] Several biophysical techniques, including solid-state NMR, have previously been used to understand the interaction between some of the MSI peptides and different model lipid membranes for the purpose of investigating the mechanism by which they cause membrane disruption.[25,28−30] Until recently, three different broadly defined mechanisms have been proposed,[31] namely, the carpet, barrel-stave, and toroidal-pore mechanisms, and evidence of such mechanisms has also been reported in the literature.[32−34] Pexiganan, or MSI-78, has been shown to function via a toroidal-pore mechanism, and at very high concentrations, it fragments the lipid bilayer.[35] Our initial studies employing multilamellar vesicles (MLVs) and aligned lipid bilayers ruled out the possibility of barrel-stave and detergent-type mechanisms.[35,36] In these studies, solid-state NMR experiments with mechanically aligned lipid bilayers were used to determine the orientation of an AMP in a membrane environment and to rule out the barrel-stave mechanism. Additionally, these studies aimed to determine the role of positive curvature induced by MSI-78 and revealed toroidal pore formation.[35] The lack of bulk water in the mechanically aligned bilayer samples and the powder pattern ^{31}P NMR spectrum observed from MLVs are not suitable for determining the detergent-type mechanism of action by an AMP. On the other hand, our recent study using large unilamellar vesicles (LUVs) demonstrated that the mechanism of membrane disruption is membrane composition-dependent: the potent AMP, MSI-78, fragmented lipid vesicles composed of zwitterionic POPC, and anionic lipids (POPG or POPS), but not the vesicles containing either zwitterionic or anionic lipid alone.[37] Though it is believed that the detergent-type membrane fragmentation could be a potent mechanism of action for many AMPs,[33,34] it is very difficult to identify this mechanism by conventional biophysical and biochemical approaches, including light scattering, dye leakage experiments,[6,19] IR, and sum frequency generation. These techniques are insensitive to the small population of lipid fragments removed from an intact membrane as a result of AMP membrane disruption. As demonstrated in our recent study, static ^{31}P solid-state NMR experiments on LUVs are unique in identifying this mechanism. In this study, we utilize this approach to determine the detergent-type mechanism of action exhibited by MSI-78 and other MSI peptides listed in Table 1, in addition to demonstrating the effect of cholesterol in suppressing this mechanism. Static ^{31}P solid-state NMR experiments on phospholipid LUVs (POPC, POPG, POPS, POPC/POPG, or POPC/POPS) were used to investigate the membrane composition-dependent mechanism of action for these peptides.

Table 1. Amino Acid Sequences of the Antimicrobial Peptides Investigated in This Study

peptide	amino acid sequence	net charge	no. of amino acid residues
MSI-78	GIGKFLKKAKKFGKAFVKILKK-NH_2	+9	22
MSI-367	KFAKKFAKFAKKFAKFAKKFA-NH_2	+9	21
MSI-594	GIGKFLKKAKKGIGAVLKVLTTGL-NH_2	+6	24
MSI-843	OCT-OOLLOOLOOL-NH_2	+6	13

MATERIALS AND METHODS

1-Palmitoyl-2-oleoyl-*sn*-glycero-3-phosphocholine (POPC), 1-palmitoyl-2-oleoyl-*sn*-glycero-3-phospho-L-serine sodium salt (POPS), and 1-palmitoyl-2-oleoyl-*sn*-glycero-3-phospho(1′-*rac*-glycerol) sodium salt (POPG) were purchased from Avanti Polar Lipids Inc. (Alabaster, AL). Chloroform and cholesterol were purchased from Sigma-Aldrich (St. Louis, MO). All MSI peptides, MSI-78, MSI-594, MSI-367, and MSI-843, used in this study were synthesized and donated by Genaera Corp. Stock solutions of the peptides were prepared in Millipore water.

Preparation of Lipid Vesicles. Lipid solutions in chloroform were dried under a stream of dry nitrogen gas and evaporated under high vacuum to dryness in a test tube. For cholesterol/lipid samples, an appropriate volume of the cholesterol stock solution solubilized in chloroform (20 mg/mL) was mixed with lipids dissolved in chloroform; the mixture was dried by a stream of N_2 gas, and then the solvent was further removed by placing the sample in a vacuum chamber at room temperature overnight. HEPES buffer [250 μL; 10 mM HEPES and 50 mM NaCl (pH 7.4)] was added into the tube and briefly vortexed, followed by extrusion through a polycarbonate filter (Nuclepore, Pleasanton, CA) mounted in a miniextruder (Avestin Inc., Ottawa, ON) fitted with two 0.5 μL Hamilton gastight syringes (Hamilton, Reno, NV) to obtain large unilamellar vesicles (LUVs) of 1.0 μm in diameter. Samples were subjected to 23 passes through two filters in tandem. An odd number of passages were performed to avoid contamination of the sample by vesicles that have not passed through the first filter. The total amount of lipid used was 8 mg for each NMR experiment. An AMP peptide solution, dissolved in water, was added to LUVs to prepare the appropriate final peptide:lipid molar ratio, making a final sample volume of 260 μL.

DOI: 10.1021/bi501418m
Biochemistry 2015, 54, 1897−1907

Samples for CD and magic angle spinning (MAS) experiments were prepared as follows. MSI-78 was dissolved at a concentration of 2 mM in an appropriate buffer and subsequently diluted to 4 or 8 mol % of the total lipid concentration of LUVs. The lipid/peptide mixture was then subjected to centrifugation at 12000 rpm for 10 min using an Eppendorf Micro centrifuge, and the resulting supernatant and pelleted fractions were separated. Figure S1 of the Supporting Information shows the lipid/peptide mixture before and after centrifugation; 75% of the supernatant was retained, whereas the pellet was subjected to three buffer washes to ensure no free MSI-78 remained in the sample. Following isolation of the supernatant and pelleted fraction, the individual samples were analyzed by CD and/or ^{1}H solution NMR or MAS solid-state NMR experiments.

NMR Experiments. ^{31}P NMR spectra were obtained on an Agilent/Varian 400 MHz solid-state NMR spectrometer operating at the resonance frequency of 400.13 MHz for ^{1}H and 161.98 MHz for ^{31}P nuclei and using a 5 mm ^{1}HX double-resonance MAS probe (Agilent/Varian). ^{31}P NMR experiments were performed using a 90° pulse width of 5 μs, 35 kHz proton decoupling, a recycle delay of 3, and 1200 scans. LUVs were put in a 5 mm glass tube, which was cut to fit into the MAS probe. All ^{31}P NMR spectra were processed using 100 Hz line broadening referenced externally to 85% phosphoric acid (0 ppm). All experiments were performed at 37 °C. ^{31}P NMR spectra of LUVs without peptide were collected first. An appropriate amount of a peptide from a stock solution in buffer was then added to LUVs, and the mixture was gently shaken before the sample was placed into the probe for NMR measurements. A temperature control unit was used to maintain the sample temperature at 37 °C. ^{31}P NMR spectra were simulated and/or deconvoluted using a FORTRAN program. The perpendicular edges in most ^{31}P NMR spectra of LUVs are well-resolved. However, the resolution at the parallel edges of the ^{31}P powder pattern spectra is poor because of the low signal-to-noise ratio, which result in large errors in the spectral simulations. ^{31}P CSA values determined from ^{31}P powder pattern NMR spectra are summarized in Table S1 of the Supporting Information.

MAS solid-state NMR experiments were performed on the pelleted fraction (see sample preparation described above) at 37 °C on an Agilent/Varian VNMRS 600 MHz solid-state NMR spectrometer using a 3.2 mm ^{1}HXY triple-resonance MAS probe. ^{1}H MAS spectra were recorded with 1000 scans and a 14 ppm spectral width under 5 or 10 kHz MAS. The proton radiofrequency carrier frequency was set at water-proton resonance for all experiments. The radiofrequency field strength used for the 90° pulses was 50 kHz.

Circular Dichroism (CD) Experiments. All CD experiments were performed on a JASCO J-1500 spectropolarimeter using a 0.1 cm path length cell. The isolated supernatant and pelleted fractions were diluted five times prior to performing CD experiments to ensure that the saturation of the detector did not occur.

RESULTS AND DISCUSSION

Fragmentation of Mixed LUVs by MSI Peptides. LUVs containing a 7:3 zwitterionic (POPC):anionic (POPS or POPG) lipid molar ratio were prepared, and ^{31}P static NMR spectra were recorded. Results obtained for POPC/POPS or POPC/POPG LUVs are shown in Figures 1 and 2, respectively. As observed previously for MSI-78,[37] a narrow peak at the isotropic chemical shift frequency (~0 ppm) appeared in the presence of almost all the MSI peptides at a peptide concentration of 2 mol %. This result alone confirms that all the MSI (78, 367, 594, and 843) peptides can disrupt lipid vesicles by the formation of small lipid aggregates via a detergent-like mechanism. The small lipid aggregates such as SUVs or micelles have a high degree of curvature that leads to fast diffusion of lipid molecules and tumbling that is sufficiently fast on the NMR time scale to average out the ^{31}P chemical

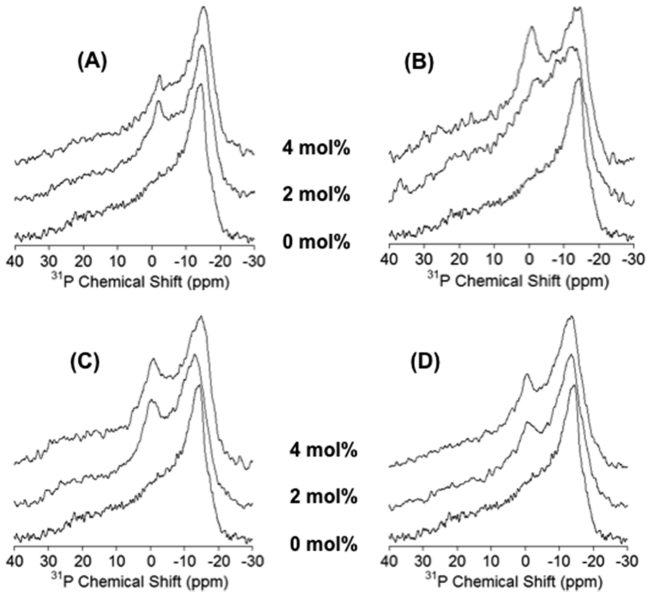

Figure 1. Static ^{31}P NMR spectra of 1000 nm large unilamellar vesicles (LUVs) composed of a mixture with a 7:3 molar ratio of zwitterionic POPC and anionic POPS lipids and MSI peptides in 10 mM HEPES buffer (pH 7.4) with 50 mM NaCl acquired at 37 °C: (A) MSI-78, (B) MSI-367, (C) MSI-594, and (D) MSI-843.

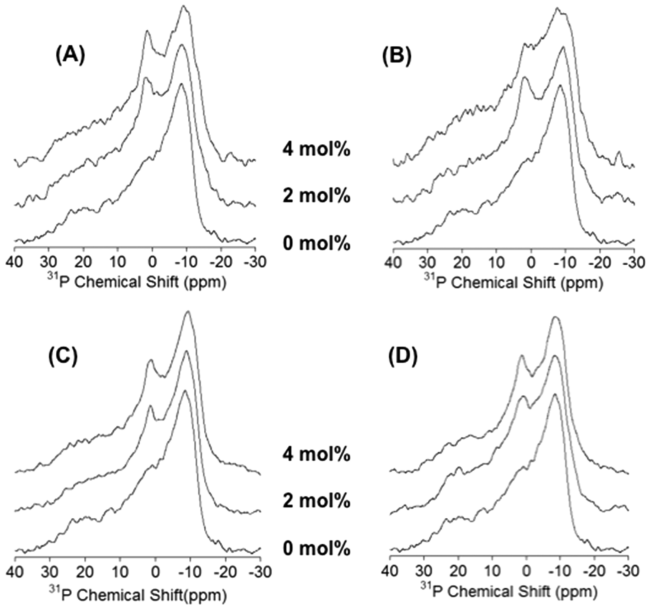

Figure 2. Static ^{31}P NMR spectra of 1000 nm large unilamellar vesicles (LUVs) constituting a mixture with a 7:3 molar ratio of zwitterionic POPC and anionic POPG lipids and MSI peptides in 10 mM HEPES buffer (pH 7.4) with 50 mM NaCl obtained at 37 °C: (A) MSI-78, (B) MSI-367, (C) MSI-594, and (D) MSI-843.

DOI: 10.1021/bi501418m
Biochemistry 2015, 54, 1897−1907

shift anisotropy (CSA) interaction, resulting in a narrow peak at the isotropic chemical shift frequency. In comparison, recent studies have made use of oriented ^{31}P NMR spectra that favor a pore model[38,39] and showed that an isotropic peak intensity may also arise from lipids in highly curved structures such as pores. The effect of PDC-109 on the DMPC MLVs also showed the fragmented small aggregates, leading to an isotropic intensity in the ^{31}P NMR spectrum.[40] Upon further titration of the MSI peptides (from 2 to 4 mol %) to LUVs, intensity changes for the isotropic peaks were observed. This could be due to the effect of the amino acid sequence of MSI peptides and, hence, their propensity to interact with the lipid vesicle. ^{31}P powder pattern spectra of the POPC/POPS LUVs in the absence of the peptides were simulated by the superposition of two axially symmetric chemical shift line shapes for POPC and POPS with CSA (chemical shift anisotropy) values of (−14.8 ppm, 25 ppm) and (−18 ppm, 30 ppm), respectively (Figure 3A). In the presence of 2 mol % MSI-78, the ^{31}P CSA values

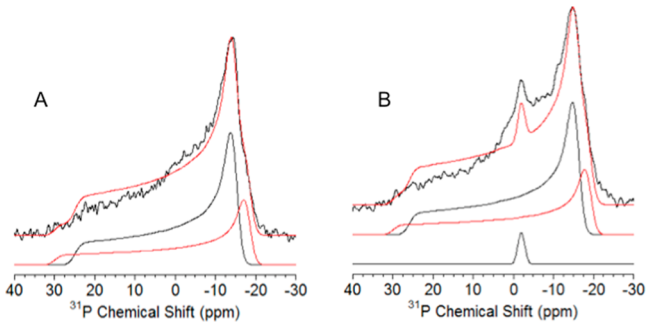

Figure 3. Experimental (black) and simulated (red) ^{31}P NMR spectra of LUVs with a 7:3 POPC:POPS molar ratio without (A) and with 2 mol % MSI-78 (B). (A) CSA values used for POPC and POPS line shapes in the simulations are (−14.8 ppm, 25 ppm) and (−18 ppm, 30 ppm), respectively, in the absence of MSI-78 (A) and (−15.8 ppm, 25 ppm) and (−18.8 ppm, 30 ppm), respectively, in the presence of 2 mol % MSI-78 (B). In addition, an isotropic component contributes 2 ± 0.5% to the total intensity in panel B.

are (−15.8 ppm, 25 ppm) and (−18.8 ppm, 30 ppm) for POPC and POPS, respectively (Figure 3B), and the isotropic intensity was ∼ 2% of the powder pattern signal intensity. Similar results were also observed when the MSI peptides were added to the LUVs containing POPC and POPG lipids at the same ratio as POPC and POPS (Figure 2). These results suggest that the interaction between the peptide and lipid bilayer is driven by electrostatic interactions as reported previously,[29,35] while the membrane fragmentation is mainly driven by the hydrophobic interaction between the peptide and lipids as discussed below. Interestingly, the difference between the anionic lipid head-groups, serine in POPS and glycerol in POPG, did not play any role in the membrane disruptive mechanism of action by the MSI peptides. This finding is important as POPS and POPG are not present in all cellular membranes and most biophysical studies utilize POPG for an anionic lipid.

With the appearance of the isotropic peak in ^{31}P NMR spectra, it is obvious that MSI peptides perturbed the lipid bilayer and formed small aggregates that tumble fast enough to result in the averaging of ^{31}P chemical shift anisotropy. To further understand the membrane disruption process, a sample of the peptide/lipid mixture (Figure 4A) was centrifuged and separated into two parts: the supernatant and pelleted fraction (Figure 4B,C and Figure S1 of the Supporting Information).

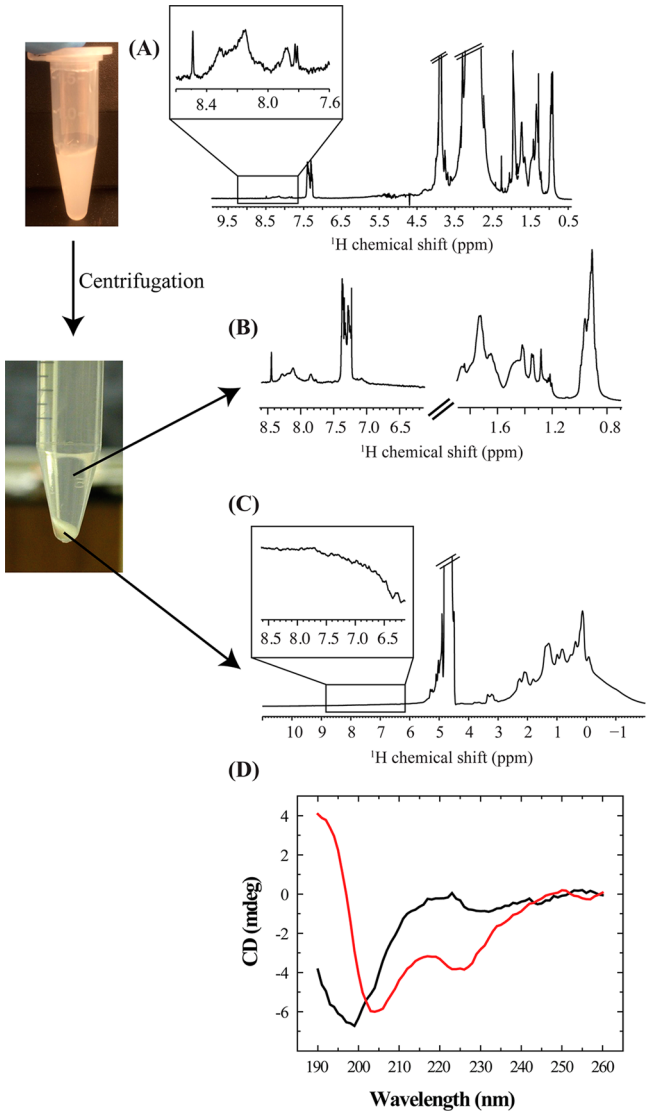

Figure 4. (A) 1D ^{1}H NMR spectrum of MSI-78 in POPC/POPS (7:3) LUVs. The experiment was performed at 37 °C using a 600 MHz Bruker NMR spectrometer. (B) Proton NMR spectrum of the supernatant solution containing MSI-78 incorporated small micelle-like lipid aggregates. The NMR experiment was performed on a Bruker Avance 600 MHz NMR spectrometer equipped with a cryoprobe at 37 °C. (C) Proton NMR spectrum of the pellet containing lipid vesicles and MSI-78 obtained at 37 °C under 10 kHz magic angle spinning conditions using an Agilent/Varian VNMRS 600 MHz solid-state NMR spectrometer. (D) Circular dichroism spectra of MSI-78 in buffer (black) or in a supernatant solution of LUVs (red).

The one-dimensional (1D) ^{1}H NMR spectrum of MSI-78 sample-containing POPC/POPS (7:3) LUVs exhibited signals from MSI-78 as well as lipids (Figure 4A). Following the separation of the two fractions, we acquired a ^{1}H NMR spectrum of the supernatant (Figure 4B and Figure S2 of the Supporting Information) and a ^{1}H MAS NMR spectrum of the pelleted fraction (Figure 4C). Interestingly, the downfield region of the ^{1}H spectrum of the supernatant solution shows broadening of proton−amide peaks (in the ∼7−9 ppm chemical shift region) originating from the MSI-78 peptide (Figure 4A and Figure S2 of the Supporting Information). Additionally, in the high-field region of the supernatant spectrum, the aliphatic peaks (∼1−2 ppm) of MSI-78 also

DOI: 10.1021/bi501418m
Biochemistry 2015, 54, 1897−1907

show broad lines (Figure 4B). The broad peaks observed from MSI-78 suggest that the peptide is bound to the lipid fragments removed from LUVs, as opposed to either MSI-78 completely bound to the LUVs or that freely tumbling in solution (Figure S2 of the Supporting Information). These observations are further confirmed through CD experiments. Close inspection of CD spectra confirms that the lipid-bound MSI-78 fragments found in the supernatant show two negative bands at ~208 and ~222 nm and one positive band at ~192 nm, indicative of the formation of a helical conformation (Figure 4D); it is worth mentioning that MSI-78 has a random coil structure in solution (Figure 4D). Given that MSI-78 forms a stable helix in DPC micelles,[41] it is more likely that the MSI-78 found in the supernatant of the lipid/peptide mixture is indeed bound to lipid because of the helicity observed in CD experiments (Figure 4D).

In addition to the analysis of the supernatant of the peptide/lipid mixture, we have analyzed the nature of MSI-78 in the pelleted LUVs. Given the large size of LUVs, any peptide bound to them would be unobservable by traditional solution NMR experiments. However, MAS solid-state NMR allows the observation of ^{1}H resonances of large proteins and lipid−protein/peptide complexes. In the case of MSI-78, our group has previously demonstrated that two-dimensional (2D) ^{1}H/^{1}H isotropic chemical shift correlation could be obtained under MAS conditions.[42] Here, we used ^{1}H MAS NMR to investigate if any MSI-78 remained in LUVs (i.e., in the pelleted fraction of the lipid/peptide mixture). The MAS spectrum shows broad peaks in the aliphatic region arising from large lipid vesicles (Figure 4B). However, we do not observe any amide resonances that would otherwise come from the presence of MSI-78 in the low-field region of the spectrum, which suggests that the amount of MSI-78 remaining in the lipid bilayer is negligibly small and beyond detection. This observation is further confirmed by analyzing the pelleted LUVs using CD experiments that showed no peptide remaining in the lipid bilayer (data not shown). These data point to the fact that all of the MSI-78 was bound to the lipid headgroup region of the lipid bilayer as reported in our previous solid-state NMR studies[35] and extracts lipids from the vesicle through a toroidal-pore mechanism for 7:3 POPC/POPS LUVs.[37] Killian and co-workers[43] studied MLVs (400−800 nm) with a 7:3 DOPC:DOPS ratio in the absence or presence of human IAPP (islet amyloid polypeptide protein, or also known as amylin) using ^{31}P NMR and light scattering techniques. They showed that human IAPP fragments MLVs by interacting with the lipid bilayer, and as a result, the MLVs convert into small lipid vesicles 50−200 nm in diameter. Such small vesicles are more dynamic and average the ^{31}P CSA further to reduce the ^{31}P line width. In this study, paramagnetic quenching experiments were conducted to test the integrity of the membrane following the disruption of the lipid bilayer induced by MSI−lipid interactions (Figure S3 of the Supporting Information). For intact LUVs, the paramagnetic ions quench only lipid molecules present in the outer-membrane leaflet, as these ions are not able to permeate the lipid bilayer. On the other hand, all lipid molecules fragmented by a detergent-like mechanism come into the proximity of the paramagnetic ions, and their signals are subsequently quenched, leaving a null in the ^{31}P NMR spectrum. Consequently, the fragments generated by the MSI-induced membrane disruption are most probably micelle-like lipid structures, as opposed to small-sized lipid vesicles.

Collectively, the results presented above suggest that irrespective of the amino acid sequence differences in the MSI peptides, all the MSI peptides investigated in this study fragment LUVs through a detergent-like mechanism of membrane disruption and the results herein support the idea that MSI peptides function via a carpet mechanism in POPC/POPG or POPC/POPS membranes.[37]

MSI-594 Disrupts Zwitterionic POPC LUVs. The initial driving force for the lipid−peptide interaction has been known to occur through electrostatic interactions of the positively charged amino acids of the MSI peptides and the negatively charged headgroups of lipids. To better understand this interaction, the LUVs of a single lipid (e.g., POPC, POPS, or POPG) were prepared and ^{31}P NMR spectra were obtained. The ^{31}P NMR powder pattern spectrum of POPC LUVs (in the absence of MSI peptides) showed a CSA span of 43 ppm and did not show any noticeable changes in the CSA in the presence of MSI-78 or MSI-367 (Figure 5). However, in the

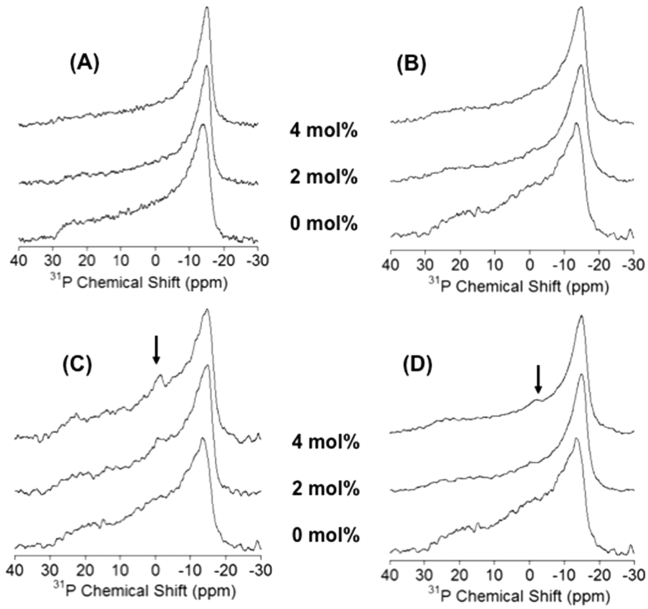

Figure 5. Static ^{31}P NMR spectra of 1000 nm large unilamellar vesicles (LUVs) containing POPC and MSI peptides in 10 mM HEPES (pH 7.4) with 50 mM NaCl acquired at 37 °C: (A) MSI-78, (B) MSI-367, (C) MSI-594, and (D) MSI-843. The arrow indicates the isotropic peaks at ~0 ppm resulting from MSI peptide-induced fragmentation of LUVs.

cases of MSI-594 and MSI-843 at 4 mol %, an isotropic peak at 0 ppm is seen (indicated by an arrow in Figure 5). Simulations of ^{31}P CSA powder pattern spectra obtained experimentally in the absence or presence of MSI peptides (MSI-78, MSI-367, and MSI-843) reveal that the relative intensities of parallel (28 ppm) and perpendicular (−15 ppm) edges of the ^{31}P line shapes have changed such that the MSI peptides caused a reduction in the intensity at the parallel edge and increased the intensity at the perpendicular edge (simulated spectra are not shown). This observation indicates that MSI-594 interacts differently with the different lipid environment, helical hairpain in LPS[27] and dynamic helix in DPC micelle.[41]

Previous studies of the membrane interaction of MSI-78 found that the peptide forms a stable antiparallel α-helical dimer and that dimer is stabilized by the formation of a Phe zipper.[40] Substitution from Phe to Gly removes the aromatic

DOI: 10.1021/bi501418m
Biochemistry 2015, 54, 1897−1907

stabilization and hence reduces the likelihood of self-aggregation in DPC micelles.[41] Interestingly, MSI-367, which contains a "Lys-Phe-Ala-Lys" repeat motif, also does not destabilize or deform the zwitterionic LUVs (Figure 5B). In contrast, MSI-594, which forms a dynamic α helix in DPC micelles,[41] can fragment the zwitterionic POPC LUVs, as confirmed by the isotropic ^{31}P NMR resonance at 0 ppm (Figure 5C). It is interesting to note that 62.5% of the amino acids of MSI-594 are hydrophobic in nature, and because of the presence of the "Gly12-Ile13-Gly14" motif in the central region of the sequence, there may be a strong hydrophobic interaction between lipid acyl chains of LUVs and the hydrophobic amino acids (Phe5, Ala9, Leu17, Val19, and Leu20) of MSI-594 that could drive the fragmentation of LUVs. MSI-843, with the interesting sequence motif Oct-Orn-Orn-Leu-Leu, shows fragmentation of POPC LUVs only at 4 mol %, and this again could be due to the strong hydrophobic interaction between acyl chains of LUVs and the Leu residues and the acyl chain component of the Orn residue in MSI-843. Taken together, the hydrophobic interaction between LUVs and residues in the peptide is likely the driving force that leads to the fragmentation of zwitterionic LUVs. While the electrostatic interaction plays a minimal role in the observed membrane fragmentation, this does not preclude electrostatic interactions from influencing binding of the peptide to the lipid bilayer (as evidenced by the changes observed in ^{31}P NMR spectra in Figure 5).

MSI-843 Disrupts Anionic POPS LUVs. The powder pattern ^{31}P NMR spectrum of POPS LUVs, with a CSA span of ~51 ppm, is shown in Figure 6. Not all MSI peptides show significant changes in the ^{31}P NMR spectra of POPS vesicles at a concentration of 2 mol %; however, at 4 mol %, we find that MSI-367 and MSI-843 induce changes to the perpendicular edge (around −15 ppm) of the ^{31}P powder pattern NMR spectra. Simulation of ^{31}P NMR spectra revealed two different CSA values of POPS for 4 mol % MSI-78 and in all samples of MSI-367 and MSI-843. The CSA values are (−16.5 ± 0.5 ppm, 35 ± 2 ppm) and (−19.8 ± 0.5 ppm, 38 ± 2 ppm) for POPS LUVs free of and treated with MSI peptides, respectively. Relative amounts of the peptide-free POPS domain decreased as the peptide concentration increased as shown in the simulated spectra for MSI-367 (Figure 7). The presence of a small peak resonating at 0 ppm for MSI-843 could be attributed to the fragmentation of LUVs. The simulated spectra indicate that, other than MSI-594, the MSI peptides alter the orientation of the lipid headgroup or shape and/or structure of POPS LUVs. The electrostatic interaction between the negatively charged POPS headgroup and the positively charged Lys residue likely serves to stabilize membrane binding yet does not induce a measurable amount of fragmentation of LUVs. In the case of MSI-843, the Orn and Leu residues are placed in such a way that in addition to the electrostatic or hydrogen bonding interactions between the NH_2 groups of the Orn residue and phosphate groups of POPS, the hydrophobic Leu residue also interacts with POPS acyl chains, which could be the main driving force for the fragmentation of lipid vesicles.

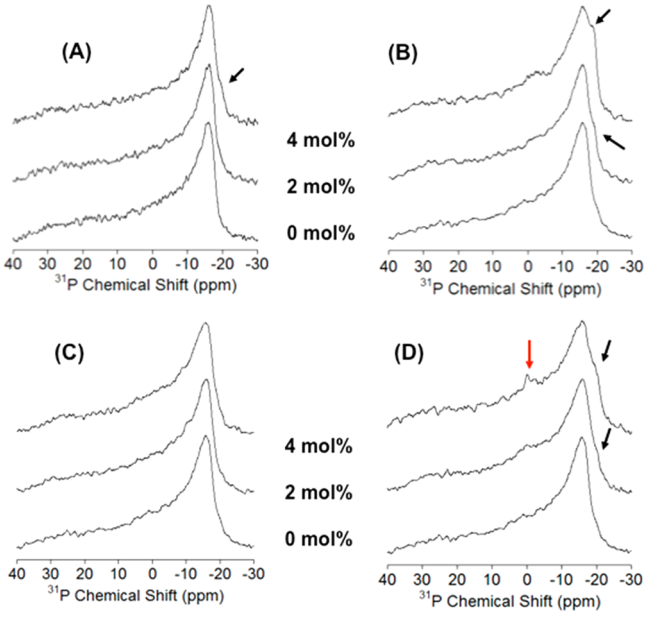

Figure 6. Static ^{31}P NMR spectra of 1000 nm LUVs containing POPS and MSI peptides in 10 mM HEPES (pH 7.4) with 50 mM NaCl obtained at 37 °C: (A) MSI-78, (B) MSI-367, (C) MSI-594, and (D) MSI-843. The arrow indicates the isotropic peaks near 0 ppm resulting from MSI peptide-induced fragmentation of LUVs. The changes in the ^{31}P NMR spectra of LUVs in the presence of either MSI-367 or MSI-843 are also marked by arrows.

MSI-594 and MSI-843 Disrupt Anionic POPG LUVs. POPG LUVs also show a powder pattern lamellar phase ^{31}P NMR spectrum (Figure 8) from LUVs that are 1 μm in diameter. However, a small isotropic intensity around 0 ppm even in the absence of MSI peptides was also observed. This is probably due to the lipid's propensity not to form perfect LUVs. Addition of MSI peptides to the POPG LUVs did show some minor changes in vesicle stability with MSI-367, MSI-843, and MSI-594 only at a high concentration (4 mol %). It is not clear from the experimental data whether these changes are due to the presence of peptides or the vesicles themselves. Instead, the ^{31}P NMR spectra of POPG LUVs revealed two different domains of POPG in the presence of MSI-78 and MSI-843. The CSA values are determined to be (−8.5 ± 0.5 ppm, 24 ± 1 ppm) and (−12 ± 0.5 ppm, 31.5 ± 1 ppm) for POPG vesicles in the absence and presence of MSI peptides, respectively. Similar to the findings of the interactions with POPS vesicles, relative amounts of peptide-free POPG domains decreased as the peptide concentration increased as shown in the simulated spectra in Figure 9.

Cholesterol Inhibits the MSI-Induced Fragmentation of LUVs. Cholesterol, when incorporated into a lipid bilayer, positions itself in the proximity of the phospholipid headgroups, and the hydrophobic chain of cholesterol interacts with lipid acyl chains and thereby acts to stabilize the lipid membrane. ^{31}P NMR spectra of 7:3 POPC/POPS LUVs containing increasing amounts of cholesterol were recorded in the presence of MSI peptides (Figures 10 and 11). Cholesterol had no apparent effect on the stability of LUVs as evidenced by the well-defined ^{31}P powder pattern NMR spectra shown in Figure 10. However, upon addition of MSI-78 to these cholesterol-containing LUVs (up to 25 mol % cholesterol), we can see the appearance of a peak close to 0 ppm in the ^{31}P NMR spectra. This indicates that the phase-sensitive cholesterol (up to 20 mol %) has no effect on the stabilization of the lipid membrane (Figure 10A,B). In contrast, as the concentration of cholesterol is increased, the intensity of the isotropic peak decreases. At the more physiological concentration of cholesterol (30 mol %), the isotropic peak did not appear even up to MSI-78 concentrations of 4 mol % (Figure

DOI: 10.1021/bi501418m
Biochemistry 2015, 54, 1897−1907

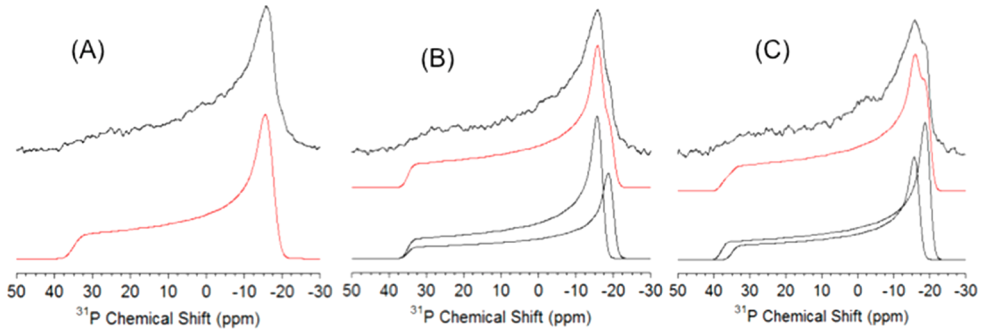

Figure 7. Experimental (topmost traces) and simulated static ^{31}P NMR spectra of POPS LUVs (A), POPS LUVs incorporated with 2 mol % MSI-367 (B), and 4 mol % MSI-367 (C). Spectrum A was simulated using CSA tensor values of (−16.5 and 35 ppm). Spectra B were simulated using two different CSA values of (−16.5 ppm, 35 ppm) and (−19.5 ppm, 35 ppm). This indicated that there MSI-367-free and MSI-367-affected POPS domains give two different CSA line shapes. Spectra C were simulated using two different CSA values of (−16.5 ppm, 35 ppm) and (−19.8 ppm, 38 ppm). The relative ratios between the two domains are 1:0.6 (B) and 0.75:1 (C).

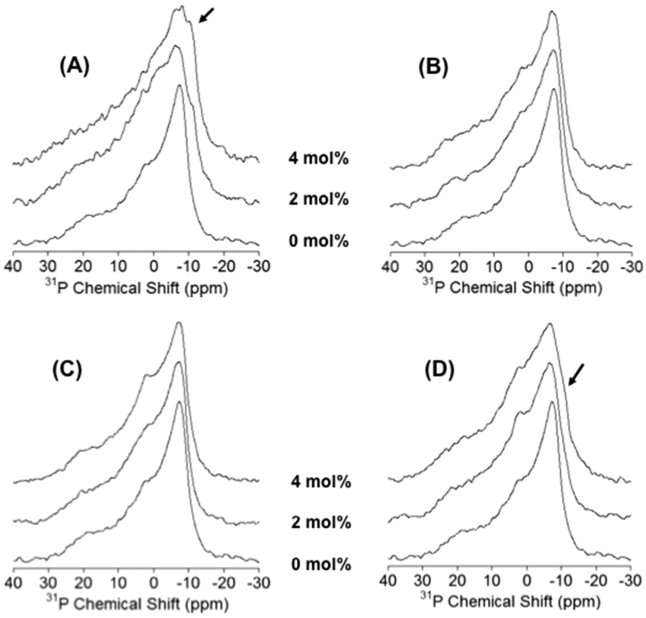

Figure 8. Static ^{31}P NMR spectra of 1000 nm POPG LUVs containing MSI peptides in 10 mM HEPES (pH 7.4) with 50 mM NaCl acquired at 37 °C: (A) MSI-78, (B) MSI-367, (C) MSI-594, and (D) MSI-843.

10D). Spectral simulations revealed that the ^{31}P CSA values of POPC and POPS in 7:3 POPC/POPS LUVs in the absence of MSI-78 were slightly reduced as the cholesterol concentration was increased from 10 to 30 mol % (see Table S1 of the Supporting Information). However, the addition of MSI-78 to LUVs did not show noticeable changes in the CSA line shape. These results confirm that cholesterol stabilizes 7:3 POPC/POPS LUVs in such a way that it inhibits the partial peptide-induced fragmentation of the membrane into small aggregates of lipids. To further characterize the nature of binding of MSI-78 to cholesterol-containing lipid vesicles, we recorded CD spectra on the fractionated sample in the same manner as explained above, centrifuging the lipid/peptide mixture into two distinct parts: supernatant and pelleted fractions. The CD spectrum of the supernatant showed a primarily random coil structure for MSI-78, suggesting that the peptide is not contained in a micelle-like lipid structure (Figure S4 of the Supporting Information). Furthermore, we observed no signal from the CD spectrum of the pelleted fraction of the cholesterol-containing membranes (data not shown). These results suggest that binding of MSI-78 to the lipid headgroup region of the lipid bilayer is reduced by the presence of cholesterol, and therefore, the peptide is mostly found in the solution phase but not in the lipid phase. These results are in agreement with ^{31}P NMR data that reveal cholesterol has a preventative effect on the disruption of the membrane by MSI-78.

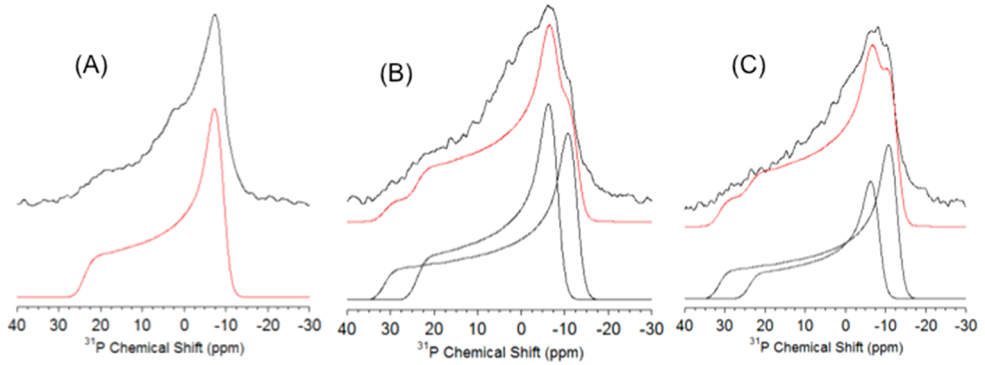

Figure 9. Experimental (topmost traces) and simulated static ^{31}P NMR spectra of POPG LUVs in the absence (A) and presence of 2 mol % MSI-78 (B) and 4 mol % MSI-78 (C) shown in Figure 6A. Spectrum A was simulated using the CSA tensor values of −8.5 and 24 ppm. Spectra B and C were simulated using two different CSA values of (−8.5 ppm, 24 ppm) for the free POPG domain and (−12 ppm, 31.5 ppm) for the MSI-78-affected POPG domain. The relative ratios between the two domains are 1:0.85 (B) and 0.65:1 (C).

DOI: 10.1021/bi501418m
Biochemistry 2015, 54, 1897−1907

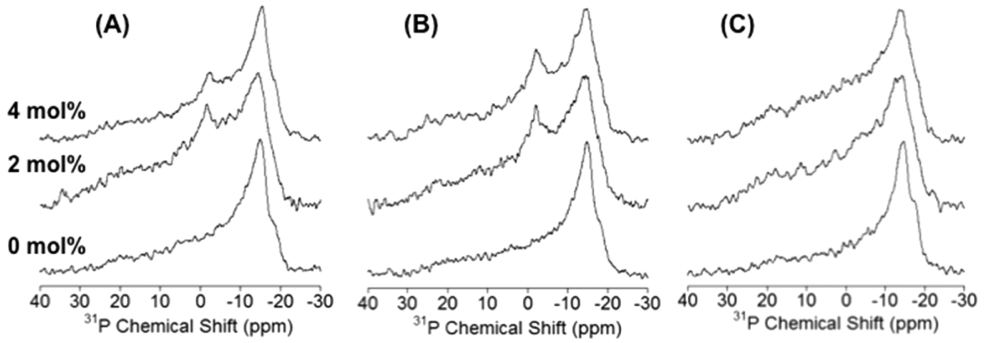

Figure 10. Static ^{31}P NMR spectra of 1000 nm 7:3 POPC/POPS LUVs containing (A) 10, (B) 20, and (C) 30 mol % cholesterol, and MSI-78 at the indicated concentration, in 10 mM HEPES (pH 7.4) with 50 mM NaCl recorded at 37 °C.

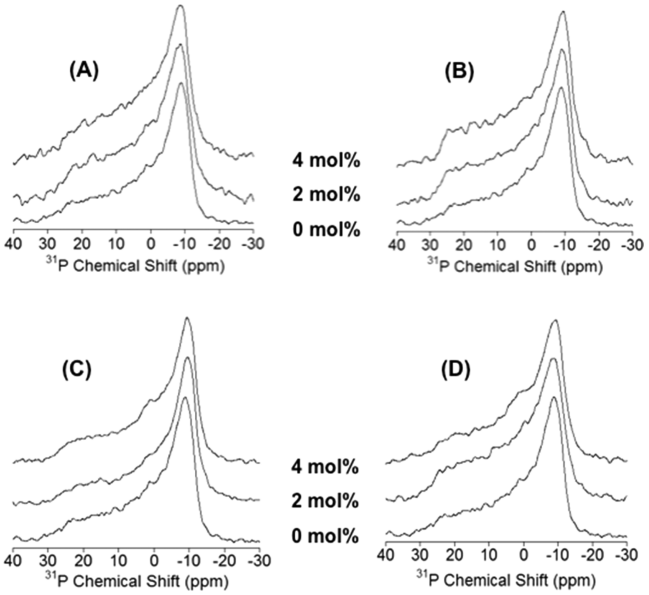

Figure 11. ^{31}P static NMR spectra of 1000 nm 7:3 POPC/POPG LUVs containing 30 mol % cholesterol, (A) MSI-78, (B) MSI-367, (C) MSI-594, and (D) MSI-843, and all the peptides at the indicated concentration, in 10 mM HEPES (pH 7.4) with 50 mM NaCl recorded at 37 °C.

A similar effect was observed in the case of POPC/POPG (7:3) LUVs containing 30 mol % cholesterol when MSI peptides were added to the lipid vesicle mixture (Figure 11). The ^{31}P NMR spectra reveal that the lipid bilayer structure of cholesterol-containing membranes is not significantly altered by the MSI peptides. Interestingly, we find that among the several MSI peptides studied only MSI-843 can fragment any type of membrane into smaller lipid aggregates, likely because of its unique amino acid sequence. Nevertheless, at a physiological level of (30 mol %) cholesterol in the membrane, MSI-843 cannot fragment the membrane. This is not surprising as Triton-X-100, a common detergent that can disrupt vesicles and cells and readily solubilizes lipids and membrane proteins, could neither disrupt nor alter the structure of lipid bilayers in the presence of 30 mol % cholesterol.[44] Table S1 of the Supporting Information summarizes the CSA values resulting from spectral simulations, in which the values did not show any noticeable changes in the presence of any of the MSI peptides (simulated spectra are not shown). A large body of literature using techniques such as DSC and solid-state NMR in conjunction with MD simulation has demonstrated the effect of cholesterol on lipid bilayer structure. One such study found that high cholesterol concentrations in eukaryotic cells inhibit membrane disruption by increasing the membrane thickness. Similar observations were reported from different groups studying POPC LUVs,[45] PE/PC monolayers,[46] and DPPC bilayer.[47] Previous studies have confirmed that the stability of lipid membranes with physiological cholesterol concentrations is well correlated with the phase of lipids, as it is well-known that high cholesterol concentrations can form a liquid order phase (Lo). Cholesterol has been shown to have protective effects against membrane disruption by amyloid-forming peptide, such as amyloid-β.[48−50]

In summary, the most potent MSI peptide, MSI-78, which forms a stable helical dimer in zwitterionic DPC micelles through the formation of a stable phenylalanine zipper,[41] could not fragment the POPC LUVs. One reason could be that the peptide is inserted into the lipid membrane and stabilized by extensive hydrophobic interactions with the acyl chains of lipid molecules, while charged residues of MSI-78 interact with the phospholipid headgroups. This reasoning can be extended to the case of LUVs of a single lipid type, whereas with LUVs with lipid mixtures, the binding affinity and membrane permeabilization could not be correlated because of the complex nature of the lipid bilayer environment. Interestingly, MSI-367 also follows a trend similar to that of MSI-78; membrane fragmentation occurs only to those LUVs of mixed lipid types. However, MSI-594 and MSI-843 fragment LUVs irrespective of whether it is a single or mixed lipid system. One explanation for this could derive from the differing amino acid sequences of the MSI peptides, especially in the case of MSI-843. The peptide is short and therefore may be highly dynamic; even when the peptide is bound to vesicles, the binding affinity could be in millimolar range. Furthermore, because of the incorporation of an acyl chain in the sequence of MSI-843, the hydrophobic interactions likely dominate electrostatic interactions and could be the governing factor for the observed membrane fragmentation of different LUVs. This membrane fragmentation is almost completely suppressed by introducing cholesterol, which serves to reduce the mobility of the membrane by increasing the degree of order in the membrane. Hence, irrespective of the MSI peptides' amino acid sequence, cholesterol inhibits fragmentation of the lipid membrane. It is also worth mentioning that the concentration of cholesterol used in this study is within the physiological range for many membranes, including the plasma membrane of erythrocytes.[51,52] Because eukaryotic cell membranes contain heterogeneous lipid systems, including cholesterol, it is thus an important arena for understanding the selectivity and toxicity of

DOI: 10.1021/bi501418m
Biochemistry 2015, 54, 1897−1907

AMPs for a better design of new, more potent AMPs to pave ways for the further development of novel antibiotics.

CONCLUSIONS

In this study, we have experimentally demonstrated the detergent-type carpet mechanism of membrane disruption by synthetically designed potent cationic MSI antimicrobial peptides that differ in amino acid sequence and net charge. Our solid-state NMR experiments on LUVs revealed the formation of MSI-induced small size, "micelle-like" lipid aggregates, containing helical MSI peptides that resulted in an isotropic chemical shift peak. Solid-state NMR results also demonstrate the ability of cholesterol to inhibit the MSI-induced membrane fragmentation by making the lipid bilayers more rigid. These results are useful in improving our understanding of the antimicrobial function of MSI peptides (MSI-78, MSI-367, MSI-594, and MSI-843) and provide insights into the role of cholesterol on the bacterial selectivity of AMPs. While the detergent-like membrane fragmentation is not easy to identify by most biophysical techniques, our solid-state NMR experiments demonstrated in this study are unique and are useful for detecting the small population of lipid−peptide complex fragmented from the large population of LUVs in the sample. We believe that this approach can be useful for investigating the cell toxicity of amyloid peptides such as amyloid-β[53] and islet amyloid polypeptide[54] that are known to interact with lipid bilayers of the target cell membrane and disrupt the membrane to kill the cells. Though NMR is not a high-throughput technique, the use of higher magnetic fields, microcoil NMR probes, the paramagnetic relaxation enhancement effect, and possibly dynamic nuclear polarization just above the gel-to-liquid crystalline phase transition temperature under slow-spinning MAS should significantly enhance the sensitivity of the solid-state NMR technique used in this study.[55−64] Therefore, with these recent developments, NMR can be used as a high-throughput technique to study cell membrane-interacting peptides such AMPs or the required peptide and lipid concentrations can be considerably lowered. It may also be mentioned here that the in-cell approaches[63,64] used in recent NMR studies could also enhance the investigation of AMPs at high resolution.

ASSOCIATED CONTENT

Supporting Information

Additional data and figures. This material is available free of charge via the Internet at http://pubs.acs.org.

AUTHOR INFORMATION

Corresponding Author

*E-mail: ramamoor@umich.edu. Telephone: (734) 647-6572.

Funding

This research was supported by funds from the National Institutes of Health (GM084018 and GM095640 to A.R.). D.-K.L. was partly supported by the Basic Science Research Program through the National Research Foundation of Korea (NRF) funded by the Ministry of Education, Science and Technology (2009-0087836).

Notes

The authors declare no competing financial interest.

ACKNOWLEDGMENTS

D.-K.L. and A.B. were on sabbatical leave from their home institutions during the investigation of this study at the University of Michigan.

ABBREVIATIONS

AMP, antimicrobial peptide; NMR, nuclear magnetic resonance; POPC, 1-palmitoyl-2-oleoyl-*sn*-glycero-3-phosphocholine; POPS, 1-palmitoyl-2-oleoyl-*sn*-glycero-3-phospho-L-serine sodium salt; POPG, 1-palmitoyl-2-oleoyl-*sn*-glycero-3-phospho-(1′-*rac*-glycerol) sodium salt; MLV, multilamellar vesicle; LUV, large unilamellar vesicle; MAS, magic angle spinning; CD, circular dichroism.

REFERENCES

(1) Zasloff, M. (2002) Antimicrobial peptides of multicellular organisms. *Nature 415*, 389−395.
(2) Hancock, R. E., and Sahl, H. G. (2006) Antimicrobial and host-defense peptides as new anti-infective therapeutic strategies. *Nat. Biotechnol. 24*, 1551−1557.
(3) Shai, Y. (1999) Mechanism of the binding, insertion and destabilization of phospholipid bilayer membranes by α-helical antimicrobial and cell non-selective membrane-lytic peptides. *Biochim. Biophys. Acta 1462*, 55−70.
(4) Nguyen, L. T., Haney, E. F., and Vogel, H. J. (2011) The expanding scope of antimicrobial peptide structures and their modes of action. *Trends Biotechnol. 29*, 464−472.
(5) Epand, R. M., and Vogel, H. J. (1999) Diversity of antimicrobial peptides and their mechanisms of action. *Biochim. Biophys. Acta 1462*, 11−28.
(6) Sani, M. A., Gagne, E., Gehman, J. D., Whitwell, T. C., and Separovic, F. (2014) Dye-release assay for investigation of antimicrobial peptide activity in a competitive lipid environment. *Eur. Biophys. J. 43*, 445−450.
(7) Li, W., Tailhades, J., O'Brien-Simpson, N. M., Separovic, F., Otvos, L., Jr., Hossain, M. A., and Wade, J. D. (2014) Proline-rich antimicrobial peptides: Potential therapeutics against antibiotic resistant bacteria. *Amino Acids 46*, 2287−2294.
(8) Lu, J. X., Blazyk, J., and Lorigan, G. A. (2006) Exploring membrane selectivity of the antimicrobial peptide KIGAKI using solid-state NMR spectroscopy. *Biochim. Biophys. Acta 1758*, 1303−1313.
(9) Bechinger, B., and Lohner, K. (2006) Detergent-like actions of linear amphipathic cationic antimicrobial peptides. *Biochim. Biophys. Acta 1758*, 1529−1539.
(10) Bhattacharjya, S., and Ramamoorthy, A. (2009) Multifunctional host-defense peptides: Functional and mechanistic insights from NMR structures of potent antimicrobial peptides. *FEBS J. 276*, 6465−6473.
(11) Matsuzaki, K., Sugishita, K., Fujii, N., and Miyajima, K. (1995) Molecular-basis for membrane selectivity of an antimicrobial peptide, magainin-2. *Biochemistry 34*, 3423−3429.
(12) Huang, H. W. (2000) Action of antimicrobial peptides: Two-state model. *Biochemistry 39*, 8347−8352.
(13) Ramamoorthy, A. (2009) Beyond NMR spectra of antimicrobial peptides: Dynamical images at atomic resolution and functional insights. *Solid State Nucl. Magn. Reson. 35*, 201−207.
(14) Bhattacharjya, S., Domadia, P. N., Bhunia, A., Malladi, S., and David, S. A. (2007) High-resolution solution structure of a designed peptide bound to lipopolysaccharide: Transferred nuclear Overhauser effects, micelle selectivity, and anti-endotoxic activity. *Biochemistry 46*, 5864−5874.
(15) Bhunia, A., Mohanram, H., Domadia, P. N., Torres, J., and Bhattacharjya, S. (2009) Designed β-boomeranag anti-endotoxic and antimicrobial peptides: Structures and activities in lipopolysaccharide. *J. Biol. Chem. 284*, 21991−21004.
(16) Japelj, B., Pristovsek, P., Majerle, A., and Jerala, R. (2005) Structural origin of endotoxin neutralization and antimicrobial activity of a lactoferrin-based peptide. *J. Biol. Chem. 280*, 16955−16961.

DOI: 10.1021/bi501418m
Biochemistry 2015, 54, 1897−1907

(17) Matsuzaki, K. (1998) Magainins as paradigm for the mode of action of pore forming polypeptides. *Biochim. Biophys. Acta 1376*, 391−400.
(18) Toraya, S., Nagao, T., Norisada, K., Tuzi, K., Saito, H., Izumi, S., and Naito, A. (2005) Morphological behavior of lipid bilayers induced by melittin near the phase transition temperature. *Biophys. J. 89*, 3214−3222.
(19) Brender, J. R., McHenry, A. J., and Ramamoorthy, A. (2012) Does cholesterol play a role in the bacterial selectivity of antimicrobial peptides? *Front. Immunol. 3*, 195−198.
(20) Porcelli, F., Buck, B., Lee, D.-K., Lee, K. J. H., Ramamoorthy, A., and Veglia, G. (2004) Structure and orientation of paradaxin determined by NMR experiments in model membranes. *J. Biol. Chem. 279*, 45815−45823.
(21) McHenry, A. J., Sciacca, M. F. M., Brender, J. R., and Ramamoorthy, A. (2012) Does cholesterol suppress the antimicrobial peptide induced disruption of lipid raft containing membranes? *Biochim. Biophys. Acta 1818*, 3019−3024.
(22) Epand, R. F., Ramamoorhty, A., and Epand, R. M. (2006) Membrane lipid composition and the interaction of paradaxin: The role of cholesterol. *Protein Pept. Lett. 13*, 1−5.
(23) Ramamoorthy, A., Lee, D. K., Narasimhaswamy, T., and Nanga, R. P. R. (2010) Cholesterol reduces paradaxin's dynamics: A barrel stave mechanism of membrane disruption investigated by solid-state NMR. *Biochim. Biophys. Acta 1798*, 223−227.
(24) Lipsky, B. A., Holroyd, K. J., and Zasloff, M. (2008) Topical virus systematic antimicrobial therapy for treating mildly infected diabetic foot ulcers: A randomized, controlled, double-blinded, multicenter trial of pexiganan cream. *Clin. Infect. Dis. 47*, 1537−1545.
(25) Gottler, L. M., and Ramamoorthy, A. (2009) Structure, membrane orientation, mechanism, and function of pexiganan: A highly potent antimicrobial peptide designed from magainin. *Biochim. Biophys. Acta 1788*, 1680−1686.
(26) Maloy, W. L., and Kari, U. P. (1995) Structure-activity studies on magainins and other host defense peptides. *Biopolymers 37*, 105−122.
(27) Bhunia, A., Ramamoorthy, A., and Bhattacharjya, S. (2009) Helical hairpin structure of a potent antimicrobial peptide MSI-594 in lipopolysaccharide micelles by NMR spectroscopy. *Chemistry 15*, 2036−2040.
(28) Domadia, P. N., Bhunia, A., Ramamoorthy, A., and Bhattacharjya, S. (2010) Structure, interactions, and antibacterial activities of MSI-594 derived mutant peptide MSI-594F5A in lipopolysaccharide micelles: Role of the helical hairpin conformation in outermembrane permeabilization. *J. Am. Chem. Soc. 132*, 18417−18428.
(29) Thennarasu, S., Huang, R., Lee, D.-K., Yang, P., Maloy, L., Chen, Z., and Ramamoorhty, A. (2010) Limiting and antimicrobial peptide to the lipid-water interface enhances its bacterial selectivity: A case study of MSI-367. *Biochemistry 49*, 10595−10605.
(30) Thennarasu, S., Lee, D.-K., Tan, A., Prasad, K. U., and Ramamoorhty, A. (2005) Antimicrobial activity and membrane selective interactions of a synthetic lipopeptide MSI-843. *Biochim. Biophys. Acta 1711*, 49−58.
(31) Shai, Y. (2002) Mode of action of membrane active antimicrobial peptides. *Biopolymers 66*, 236−248.
(32) Matsuzaki, K. (1999) Why and how are peptide-lipid interactions utilized for self-defense? Maganins and tachyplesins as archetypes. *Biochim. Biophys. Acta 1462*, 1−10.
(33) Ramamoorthy, A., Thennarasu, S., Lee, D.-K., Tan, A., and Maloy, L. (2006) Solid-state NMR investigation of the membrane disrupting mechanism of antimicrobial peptides MSI-78 and MSI-594 derived from magainin 2 and melittin. *Biophys. J. 91*, 206−216.
(34) Bechinger, B., and Lohner, K. (2006) Detergent-like actions of linear amphipathic cationic antimicrobial peptides. *Biochim. Biophys. Acta 1758*, 1529−1539.
(35) Hallock, K. J., Lee, D.-K., and Ramamoorthy, A. (2003) MSI-78, an analogue of the magainin antimicrobial peptides, disrupts lipid bilayer structure via positive curvature strain. *Biophys. J. 84*, 3052−3060.
(36) Mecke, A., Lee, D.-K., Ramamoorthy, A., Orr, B. G., and Holl, M. M. B. (2005) Membrane thinning due to antimicrobial peptide binding: An atomic force microscopy study of MSI-78 in lipid bilayers. *Biophys. J. 89*, 4043−4050.
(37) Lee, D.-K., Brender, J. R., Sciacca, M. F. M., Krishnamoorthy, J., Yu, C., and Ramamoorthy, A. (2013) Lipid composition-dependent membrane fragmentation and pore-forming mechanisms of membrane disruption by pexiganan (MSI-78). *Biochemistry 52*, 3254−3263.
(38) Kim, C., Spano, J., Park, E.-K., and Wi, S. (2009) Evidence of pores and thinned lipid bilayers induced in oriented lipid membranes interacting with the antimicrobial peptides, magainin-2 and aurein-3.3. *Biochim. Biophys. Acta 1788*, 1482−1496.
(39) Bertelsen, K., Dorosz, J., Hansen, S. K., Nielsen, N. C., and Vosegaard, T. (2012) Mechanisms of peptide-induced pore pore formation in lipid bilayers investigated by oriented ^{31}P solid-state NMR spectroscopy. *PLoS One 7*, e47745.
(40) Damai, R. S., Sankhala, R. S., Anbazhagan, V., and Swamy, M. J. (2010) ^{31}P NMR and AFM studies on the destabilization of cell and model membranes by the major bovine seminal plasma protein, PDC-109. *IUBMB Life 62*, 841−851.
(41) Porcelli, F., Buck-Koehntop, B. A., Thennarasu, S., Ramamoorthy, A., and Veglia, G. (2006) Structures of the dimeric and monomeric variants of magainin antimicrobial peptides (MSI-78 and MSI-594) in micelles and bilayers, determined by NMR spectroscopy. *Biochemistry 45*, 5793−5799.
(42) Ramamoorthy, A., and Xu, J. (2013) 2D ^{1}H/^{1}H RFDR and NOESY NMR experiments on a membrane-bound antimicrobial peptide under magic angle spinning. *J. Phys. Chem. B 117*, 6693−6700.
(43) Khemtemourian, L., Domenech, E., Doux, J. P. F., Koorengevel, M. C., and Killian, J. A. (2011) Low pH acts as inhibitor of membrane damage induced by human islet amyloid polypeptide. *J. Am. Chem. Soc. 133*, 15598−15604.
(44) Tamba, Y., Tanaka, T., Yahagi, T., Yamashita, Y., and Yamazaki, M. (2004) Stability of giant unilamellar vesicles and large unilamellar vesicles of liquid-ordered phase membranes in the presence of Triton X-100. *Biochim. Biophys. Acta 1667*, 1−6.
(45) Drolle, E., Kucerka, N., Hoopes, M. I., Choi, Y., Katsaras, J., Karttunen, M., and Leonenko, Z. (2013) Effect of melatonin and cholesterol on the structure of DOPC and DPPC membranes. *Biochim. Biophys. Acta 1828*, 2247−2254.
(46) Diakowski, W., Ozimek, L., Bielska, E., Bem, S., Langner, M., and Sikorski, A. F. (2006) Cholesterol affects spectrin-phospholipid interactions in a manner different from changes resulting from alterations in membrane fluidity due to fatty acyl chain composition. *Biochim. Biophys. Acta 1758*, 4−12.
(47) McMullen, T. P., and McElhaney, R. N. (1995) New aspects of the interaction of cholesterol with dipalmitoylphosphatidylcholine bilayers as revealed by high sensitivity differential scanning calorimetry. *Biochim. Biophys. Acta 1234*, 90−98.
(48) Yip, C. M., Elton, E. A., Darabie, A. A., Morrison, M. R., and McLaurin, J. (2001) Cholesterol, a modulator of membrane-associated Aβ-fibrillogenesis and neurotoxicity. *J. Mol. Biol. 311*, 723−734.
(49) Lin, M. C., and Kagan, B. L. (2002) Electrophysiologic properties of channels induced by Aβ25−35 in planar lipid bilayer. *Peptides 23*, 1215−1228.
(50) Di Scala, C., Chahinian, H., Yahi, N., Garmy, N., and Fantini, J. (2014) Interaction of Alzheimer's β-amyloid peptides with cholesterol: Mechanistic insights into amyloid pore formation. *Biochemistry 53*, 4489−4502.
(51) Demel, R. A., and De Kruyff, B. (1976) The function of sterols in membranes. *Biochim. Biophys. Acta 457*, 109−132.
(52) Yeagle, P. L. (1985) Cholesterol and the cell membrane. *Biochim. Biophys. Acta 822*, 267−287.
(53) Sciacca, M. F. M., Kotler, S. A., Brender, J. R., Chen, J., Lee, D.-K., and Ramamoorthy, A. (2012) Two-step mechanism of membrane disruption by Aβ through membrane fragmentation and pore formation. *Biophys. J. 103*, 702−710.

DOI: 10.1021/bi501418m
Biochemistry 2015, 54, 1897−1907

(54) Brender, J. R., Salamekh, S., and Ramamoorthy, A. (2012) Membrane disruption and early events in the aggregation of the diabetes related peptide IAPP from a molecular perspective. *Acc. Chem. Res. 45*, 454−462.
(55) Fujiwara, T., and Ramamoorthy, A. (2006) How far can the sensitivity of NMR be increased? *Annu. Rep. NMR Spectrosc. 58*, 155−175.
(56) Wickramasinghe, N. P., and Ishii, Y. (2006) Sensitivity enhancement, assignment, and distance measurement in C-13 solid-state NMR spectroscopy for paramagnetic systems under fast magic angle spinning. *J. Magn. Reson. 181*, 233−243.
(57) Linser, R., Chevelkov, V., Diehl, A., and Reif, B. (2007) Sensitivity enhancement using paramagnetic relaxation in MAS solid-state NMR of perdeuterated proteins. *J. Magn. Reson. 189*, 209−216.
(58) Yamamoto, K., Xu, J., Kawulka, K. E., Vederas, J. C., and Ramamoorthy, A. (2010) Use of a copper-chelated-lipid speeds up NMR measurements from membrane proteins. *J. Am. Chem. Soc. 132*, 6929−6931.
(59) Yamamoto, K., Vivekanandan, S., and Ramamoorthy, A. (2011) Fast NMR data acquisition from bicelles containing a membrane-associated peptide at natural-abundance. *J. Phys. Chem. B 115*, 12448−12455.
(60) Tang, M., Berthold, D. A., and Rienstra, C. M. (2011) Solid-State NMR of a large membrane protein by paramagnetic relaxation enhancement. *J. Phys. Chem. Lett. 2*, 1836−1841.
(61) Yamamoto, K., Caporini, M. A., Im, S. C., Waskell, L., and Ramamoorthy, A. (2013) Shortening spin-lattice relaxation using a copper-chelated lipid at low-temperatures: A magic angle spinning solid-state NMR study on a membrane-bound protein. *J. Magn. Reson. 237*, 175−181.
(62) Lee, M., and Hong, M. (2014) Cryoprotection of lipid membranes for high-resolution solid-state NMR studies of membrane peptides and proteins at low temperature. *J. Biomol. NMR 59*, 263−277.
(63) Yamamoto, K., Caporini, M. A., Im, S. C., Waskell, L., and Ramamoorthy, A. (2015) Cellular solid-state NMR investigation of a membrane protein using dynamic nuclear polarization. *Biochim. Biophys. Acta 1848*, 342−349.
(64) Jakdetchai, O., Denysenkov, V., Becker-Baldus, J., Dutagaci, B., Prisner, T. F., and Glaubitz, C. (2014) Dynamic nuclear polarization-enhanced NMR on aligned lipid bilayers at ambient temperature. *J. Am. Chem. Soc. 136*, 15533−15536.

DOI: 10.1021/bi501418m
Biochemistry 2015, 54, 1897−1907